Available online at http://ajol.info/index.php/ijbcs

Int. J. Biol. Chem. Sci. 6(1): 529-542, February 2012

ISSN 1991-8631

Original Paper

http://indexmedicus.afro.who.int

An investigation of the elements of the photodecomposition of Zn_xCd_{1-x} Se quantum dot

Nche George NDIFOR-ANGWAFOR and Solomon Gabche ANAGHO*

Department of Chemistry, Faculty of Science, University of Dschang, Cameroon.
** Corresponding author, Tel: +237 7757 8567, P.O. Box 814, Bamenda, North-West Region, Cameroon.*
E-mail: sg_anagho@yahoo.com

ABSTRACT

High quality $Zn_xCd_{1-x}Se$ quantum dots useful for medical imaging were synthesised by high temperature or embryonic nuclei-induced alloying technique by incorporating varying amounts of Zn precursor into CdSe nuclei. The prepared $Zn_xCd_{1-x}Se$ nanoparticles were digested in acid and the amount of metal ions present in the solution were determined by electroanalysis and AAS techniques. It was found that the Cd to Zn ratio in the prepared nanoparticles matched that present in the reaction solution. A UV-vis and HR-TEM analyses of the quantum dots showed that the Zn-Cd-Se nanoparticles were nearly mono dispersed, had well resolved lattice fringes and remained fully crystalline upon zinc incorporation. As the zinc content increased from 0.25 to 0.67, the nanoparticle size increased from 5.8 nm to 7.5 nm, and the colour of the solution varied from brown to blue. Upon tuning the quantum dots by photodecomposition, in order to produce materials suitable for biomedical imaging applications, it was observed that the nanoparticles remained crystalline, the particles sizes were reduced to a uniform size, and its solution remained permanently blue, while the absorption wavelength remained in the low wavelength region.

Keywords: Cadmium zinc selenide, embryonic nuclei induced, photodecomposition, atomic absorption spectroscopy, stripping voltammetry, nanocrystals.

INTRODUCTION

Colloidal semiconductor nanocrystals, also referred to as quantum dots (QDs) have attracted great attention for their distinguished role in fundamental studies and technical applications (Zhong et al, 2004) such as light emitting devices (Colvin et al, 1994; Gao et al, 2000; Schlamp et al, 1997; Tesser et al., 2002), lasers (Artemyev et al, 2001; Klimov et al, 2000) and biological labels (Bruchez et al, 1998; Chan et al, 1998; Jaiswal et al, 2003; Wu et al, 2003). Owing to their unique size-dependent photoluminescence tuneable across the visible spectrum, CdSe nanocrystals have become the most extensively investigated QDs (Murray et al, 1993; Peng et al, 2001; Peng, 2002; Qu et al, 2001; Qu et al, 2002).

A major problem encountered over the years in fabricating high-quality QDs is associated with the issue of precursor materials. This concerns primarily the tendency to form defects and surface-trap states under the employed growth conditions, resulting in low luminescence, low efficiency

DOI : http://dx.doi.org/10.4314/ijbcs.v6i1.47

and stability deficits. Surface-passivation of the CdSe nanocrystals with suitable organic or inorganic materials can minimise this problem by removing the non radiative recombination centres (Kippeng et al, 2008 and Kovalevskij et al, 2004).

In the last two decades, the main focus has been on the preparation of different colour-emitting QDs with different particle sizes. Little attention has been paid to the fact that different colour emitting QDs can also be made through the control of constituent stoichiometries in alloy nanoparticles. Recent advances have led to the exploration of composition-tuneable emission by changing their constituent stoichiometries in the ternary composite nanocrystals (Harrison et al, 2000; Korgel et al, 2000; Kulkarni et al, 2001; Petrov et al, 2002; Wang et al, 2002 and Yu et al, 2003).

Along similar lines, medical researchers are developing these materials for use in biomedical imaging applications. Human tissue is permeable to far infra-red light. By injecting appropriately prepared $Zn_xCd_{1-x}Se$ quantum dots having a wavelength $\leq$ 450 nm into injured tissues, it may be possible to image the tissue in those injured areas (Chan and Nie, 1998, Bruchez et al., 1998).

In this work we combined embryonic nuclei-induced alloying and photodecomposition techniques to demonstrate the production of high quality $Zn_xCd_{1-x}Se$ quantum dots with the required UV vis wavelength $\leq$ 450 nm for use in biomedical imaging.

MATERIALS AND METHODS

Chemicals

Trioctylphosphine oxide (TOPO, 90%), trioctylphosphine (TOP, 90%), hexadecylamine (HDA, 90%), stearic acid (95%), and selenium powder (99.999%) were purchased from Aldrich. Cadmium acetate (anhydrous, 99.99+%, ChemPur), n-tetradecylphosphonic acid (TDPA, 98%, AlfaAesar), diethyl zinc (95%, Strem), acetone (HPLC, Rathborne), methanol (HPLC, Rathborne), chloroform (HPLC, Rathborne), and methyl viologen (98%) were also purchased. All the chemicals were used as received from the suppliers.

Equipment

Photon technology international monochromator, Model 101/102, Perkin Elmer Lambda Bio 10 UV-Vis spectrophotometer, FEG JEOL 6300 Field Emission Scanning Microscope, Oxford Instrument ISIS 310 X-ray system, EG&G Princeton Applied Potentiostat/Galvanostat model 270, with saturated calomel electrode, and Atomic absorption spectrometer (Unicam 919 from Unicam Cambridge,UK).

Synthesis of $Zn_xCd_{1-x}Se$ Nanoparticles

Cadmium acetate (0.023 g, 0.1 mmol), stearic acid (0.11 g, 0.4 mmol), TOPO (2.0 g) and HDA (2.0 g) were loaded into a 50 ml three necked round-bottom flask. The mixture was dried and degassed in the reaction vessel by heating to 100 ^oC for 1 hour while flushing the reaction system periodically with a flow of argon. The process of flushing with argon was done 3 times. After 1 hour the reaction temperature was further increased and stabilized at 320 ^oC with stirring under a continuous flow of argon. 1.0 ml solution of Se (0.039 g, 0.5 mmol) in TOP was swiftly injected into the reaction flask. To this reaction mixture was then added 1.0 ml solution of diethyl zinc (0.2 mmol) in TOP as soon as possible (about 10 s after the addition of Se solution). The temperature was set at 310 ^oC for the subsequent growth and annealing process of the nanocrystals. After 10 minutes the round bottom flask was gently removed from the heating source and its contents gradually poured into cold chloroform (25 ^oC) to terminate any further growth of the nanocrystals.

$Zn_xCd_{1-X}Se$ particles were prepared using different ratios of Zn:Cd in the reaction vessel. This was achieved by simply changing the volumes of the 0.2 mmol diethyl zinc solution in TOP that was added to the reaction mixture. The nanoparticles were prepared using Zn:Cd ratios of 0.4, 0.8, 1.2 and 2. The resulting particles were referred to as $Zn_{0.25}Cd_{0.75}Se$, $Zn_{0.44}Cd_{0.56}Se$, $Zn_{0.56}Cd_{0.44}Se$ and $Zn_{0.67}Cd_{0.33}Se$ respectively.

Purification of Nanoparticles

The $Zn_xCd_{1-x}Se$ nanoparticles were purified by precipitation with a mixture of equal amounts of acetone and methanol and allowed to settle by gravity. To make sure that all the reaction precursors were completely removed, the process of separation with a mixture of acetone and methanol and re-suspension in chloroform was repeated three times. The pure nanoparticles obtained were dried on a hot plate at 60 ^oC in a fume cupboard.

Procedure of Photodecomposition of $Zn_xCd_{1-x}Se$ Nanoparticles

0.03 g of the dried $Zn_xCd_{1-x}Se$ nanocrystals was dissolved in 15 ml chloroform, and 5.0 ml of the solution was diluted to 30.0 ml with chloroform in a white capped vial. Methyl viologen (98%) was dissolved in methanol and added to the suspension to yield a total concentration of 10^{-5} M of viologen ions (MV^{2+}). The suspension was saturated with oxygen and then irradiated for 10 minutes with a light source from the monochromator set at 0.45 watts. Distilled water in a similar white capped vial was placed in front of the vial containing the suspension in order to absorb the heat produced and allow only UV light to pass through. This also reduced the rate of evaporation of the chloroform in the $Zn_xCd_{1-x}Se$ nanocrystals suspension. After 10 minutes there was a change in the colour of the solution. The UV absorption of these suspensions was carried out on the UV-Vis spectrophotometer.

Digestion

High purity concentrated nitric acid (2.0 ml) was added to a designed safety tube containing dry quantum dots and the resulting solution was allowed to stand overnight. Six drops of high purity concentrated hydrochloric acid was added to the tube. It was heated on a hot plate set at 80 ^oC for about 2 hours until the solution became clear and contained no more solids. The tube was designed in such a way that the toxic H_2Se vapour released was forced by argon gas into a concentrated mixture of NaOH and $ZnCl_2$ solutions. This produced ZnSe that was less toxic and in a form that could be safely disposed of. The digested solution was then diluted for cadmium and zinc ion analysis.

Analytical Protocol to Determine the Composition of $Zn_xCd_{1-x}Se$ Nanocrystals

Concentration of Zn^{2+} in $Zn_xCd_{1-x}Se$ Nanocrystals

The concentrations of zinc ions in aliquots of the digested solutions of $Zn_xCd_{1-x}Se$ nanocrystals were determined using electrochemical analysis (ECA) and atomic absorption spectroscopy (AAS, UNICAM919, Cambridge, UK). Anodic stripping voltammograms were recorded at a scan rate of 20 mVs^{-1} and deposition time of 80 s at different applied potentials relative to a saturated calomel reference. Different volumes of standard zinc nitrate solution (0.05 mol dm^{-3}) were added to the cell to give a range of concentrations of zinc ions. The voltammograms obtained were analysed to give the peak area (charge) associated with stripping the zinc deposited. The charge required to strip the zinc was then plotted against the Zn^{2+} ion concentration. This gave a linear relationship relating charge, or area under each voltammogram to the Zn^{2+} ion concentration (Figure 1)**.** Aliquots of samples taken from the digested solutions were

analysed for Zn^{2+}. The charge under the stripping peak was determined and the calibration graph used to calculate the Zn^{2+} concentration as shown in Equation 2-1.

$$x = \frac{y}{20199} \quad \text{…….(2-1)}$$

Where y = Charge below the stripping peak in the voltammogram, and

x = Zinc concentration in the solution.

The zinc ion concentrations were those of Zn^{2+} present in the cell used for the analysis. To get the actual concentration of zinc in the aliquots (and hence in the samples), the concentration of Zn^{2+} in the cell was multiplied by a dilution factor, DF given by Equation 2.2.

$$DF = \frac{V_{NaCl} + V_{HgCl_2} + V_{Zn(NO_3)_2}}{V_{Zn(NO_3)_2}} \quad \text{…..(2.2)}$$

In the AAS method a zinc calibration was obtained (Figure 2), using solutions of known concentrations prepared by dilution of a 1000 ppm standard zinc solution.

Concentration of Cd^{2+} ion in $Zn_xCd_{1-x}Se$ Nanocrystals

The same procedure as in the determination of Zn^{2+} ion in the section above was used to determine the concentration of Cd^{2+} ions in the nanocrystals. The linear relationship relating charge or area under each voltammogram to the Cd^{2+} ion concentration is given in Figure 3.

The charge under the stripping peak was determined and the calibration graph used to calculate Cd^{2+} ion concentration by using Equation 2-3.

$$x = \frac{y}{19995} \quad \text{……..(2.3)}$$

Where y = Charge or area below each voltammogram, and

x = Cadmium ion concentration that caused the voltammogram.

The cadmium ion concentrations were those of Cd^{2+} present in the cell used for the analysis. To get the actual concentration of cadmium in the samples, the concentration of the Cd^{2+} in the cell was multiplied by a dilution factor (DF) given by Equation 2-4.

$$DF = \frac{V_{NaCl} + V_{HgCl_2} + V_{Cd(NO_3)_2}}{V_{Cd(NO_3)_2}} \quad \text{….(2.4)}$$

A similar procedure as for the Zn^{2+} concentration was also used to determine the cadmium ion concentration by the AAS technique using the linear relationship from Figure 4.

Analytical Protocol to Determine the Composition of Photodecomposed Nanoparticles

A mixture containing 5.0 ml each of acetone and methanol was used to precipitate 10.0 ml of purified $Zn_xCd_{1-x}Se$ nanocrystals from a mixture of nanocrystals and methyl viologen that had been exposed to light. This precipitated the nanocrystals, and the organic layer was carefully separated from the nanocrystals. 5.0 ml of distilled water was added to the organic layer and the resulting mixture shaken and separated with the aid of a separating funnel. The separation gave an aqueous phase and an organic phase. The organic phase was placed on a hot plate set at 70 ^{o}C to evaporate off the solvent. A mixture of the $Zn_xCd_{1-x}Se$ recovered from the organic phase, and the one obtained by precipitation was digested in 5.0 ml of nitric acid and analysed using both electrochemical analysis and atomic absorption spectroscopy. The nanocrystals obtained from the aqueous phase were also similarly analysed.

In the control experiment, there was neither addition of methyl viologen to the purified $Zn_xCd_{1-x}Se$ nanocrystals nor exposure to light.

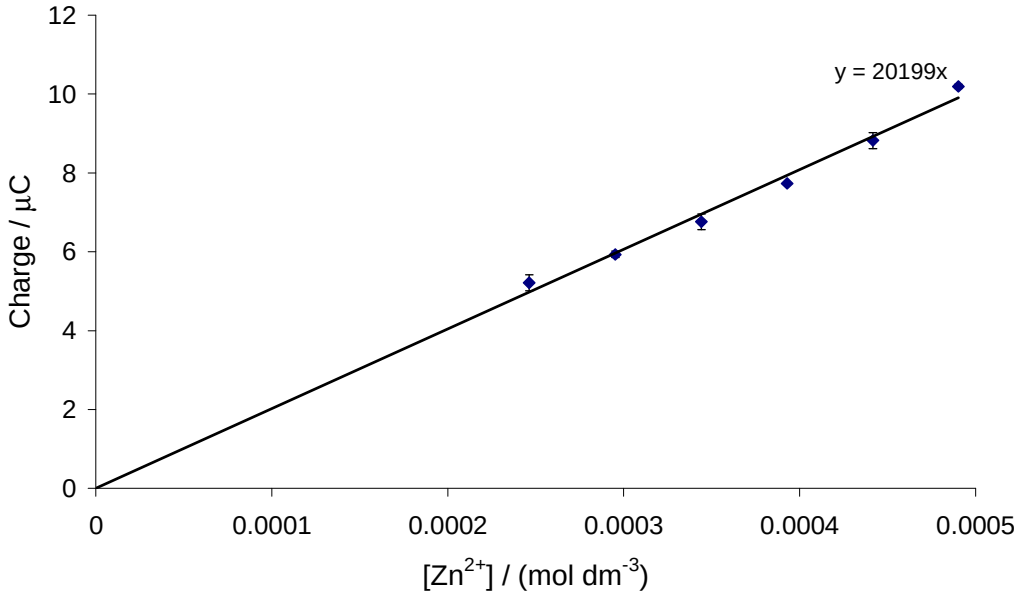

Figure 1: Standard zinc calibration curve by the electro-analytical method using different zinc ion concentration and fixed mercury ion concentration. The curve gives a linear relationship in which zinc ion concentration in the analysis cell can be calculated by dividing the charge obtained by 20199.

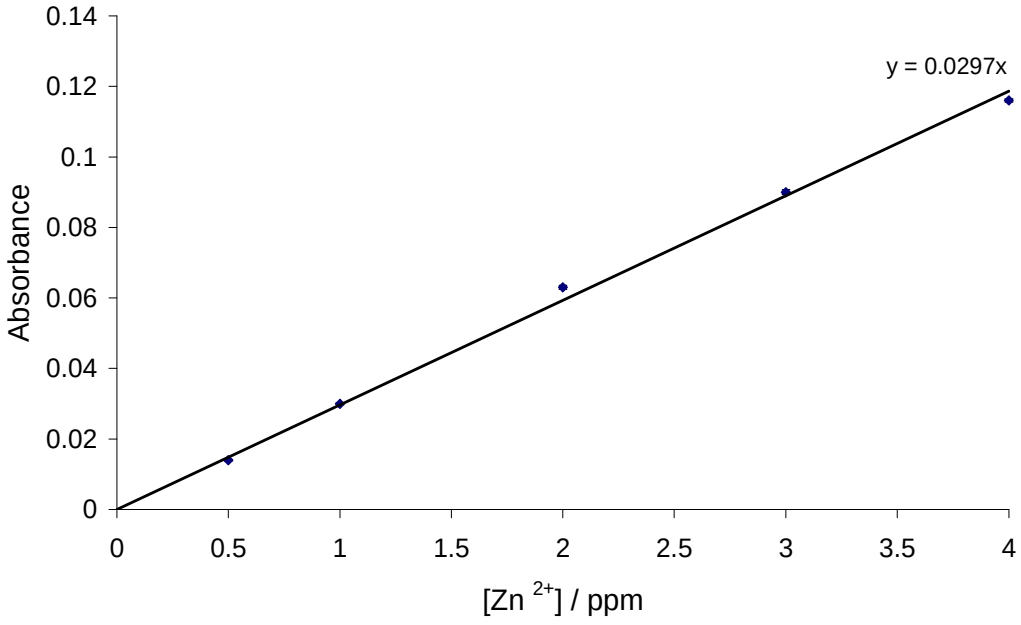

Figure 2: Standard zinc calibration curve by the AAS method using known zinc concentrations. The curve gives a linear relationship in which the concentration of zinc in the analysis solution can be calculated by dividing the absorbance obtained by 0.0297.

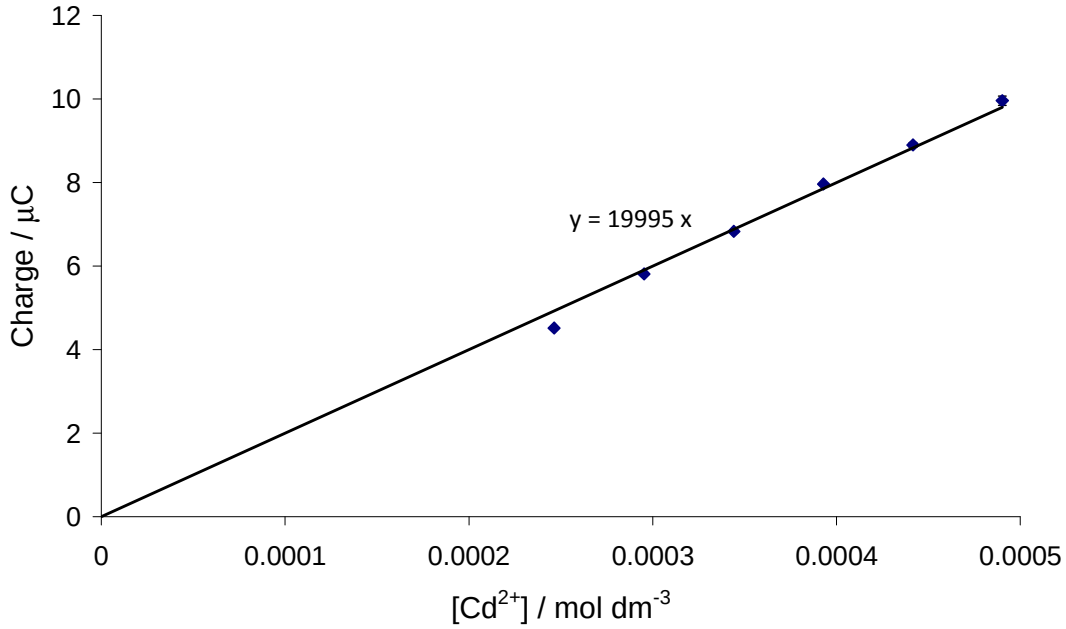

Figure 3: Standard cadmium calibration curve by the electro analytical method using different cadmium ion concentration and fixed mercury ion concentration. The curve gives a linear relationship in which cadmium ion concentration in the analysis cell can be calculated by dividing the charge obtained by 19995.

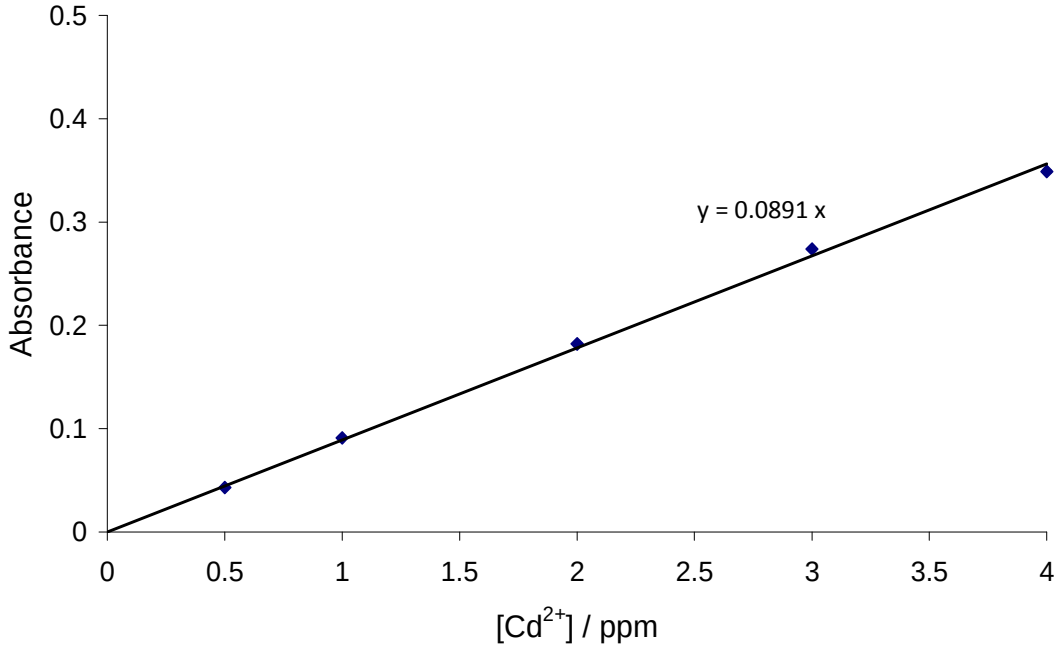

Figure 4: Standard cadmium calibration curve by the AAS method using known cadmium concentrations. The curve gives a linear relationship in which the concentration of cadmium in the analysis solution can be calculated by dividing the absorbance obtained by 0.0891.

RESULTS

UV- Vis Spectroscopy

The UV-Visible absorption spectra of the prepared $Zn_xCd_{1-x}Se$ nanocrystals are shown in Figure 5. The shift of maximum absorption to lower wavelength is due to the increasing concentration of zinc in the nanocrystal.

The UV-Visible absorption spectra of the $Zn_xCd_{1-x}Se$ nanocrystals after photodecomposition study is shown in Figure 6. The shift in the maximum absorption to lower wavelengths shows that the photoetching process gives rise to smaller particles. This indicates that photoetching is very suited for tuning the size of semiconductor nanoparticles.

Transmission Electron Microscopy

The HR-TEM of the different $Zn_xCd_{1-x}Se$ nanocrystals prior to photodecomposition is shown in Figure 7. The HR-TEM result show that the nearly mono-dispersed $Zn_xCd_{1-x}Se$ nanocrystals have well-resolved lattice fringes, and that they remain fully crystalline upon zinc incorporation. The particle size as determined by TEM increases proportionately from about 5.8 ± 0.3 to 7.5 ± 0.5 nm with an increase in the zinc content from 0.25 to 0.67. Figure 8 displays the energy dispersive x-ray spectra of the $Zn_xCd_{1-x}Se$ nanocrystals showing the presence of cadmium, zinc and selenium in the nanocrystals.

Zinc and Cadmium ions in $Zn_xCd_{1-x}Se$ Nanoparticles

The zinc and cadmium contents of $Zn_xCd_{1-x}Se$ nanoparticles were determined using AAS and electroanalytical techniques. Table 1 gives the experimentally determined Zn:Cd ratio of the nanoparticles before photodecomposition, while Table 2 gives the Zn:Cd ratio of the same set of particles after photodecomposition. The Cd:Zn ratios of the solution phase prior to decomposition are also quoted. The results of control experiments for the photodecomposition process are shown in Table 3.

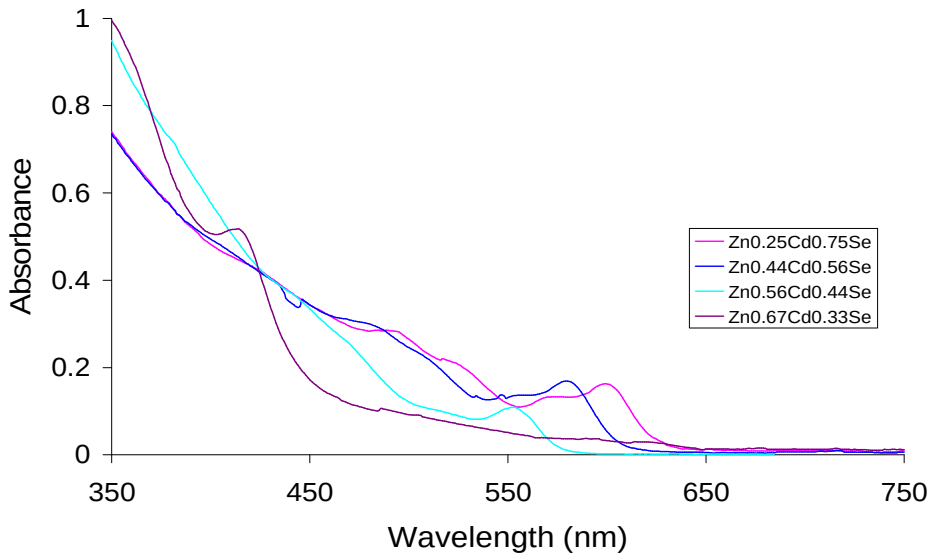

Figure 5: UV-Vis absorption spectra of the as-prepared $Zn_xCd_{1-x}Se$ prior to photodecomposition.

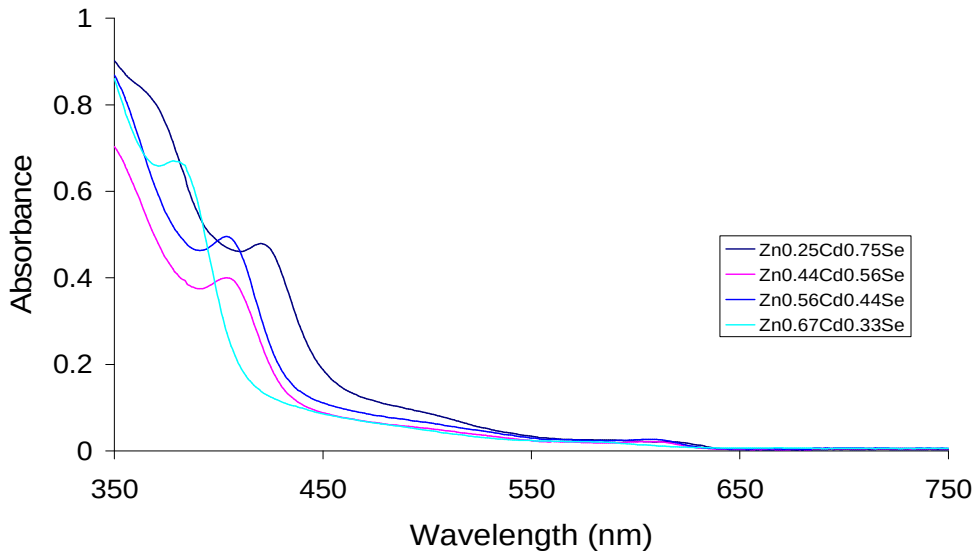

Figure 6: UV-Vis absorption of $Zn_xCd_{1-x}Se$ nanocrystals after photodecomposition showing a shift in maximum absorption to shorter wavelengths. The mole fractions shown are those present in the preparation of the alloyed $Zn_xCd_{1-x}Se$ nanocrystals before etching.

Table 1: Molar ratios of zinc and cadmium in the solution used to prepare $Zn_xCd_{1-x}Se$ nanocrystals before photodecomposition studies measured by the atomic absorption spectroscopy (AAS) and the mercury film electrochemical technique (ECA).

Zn:Cd ratio	Zn:Cd ratio in preparation	Zn:Cd molar ratio of as-prepared particles by AAS	Zn:Cd molar ratio of as-prepared particles by ECA
$Zn_{0.25}Cd_{0.75}Se$	0.4	0.3656	0.4043
$Zn_{0.44}Cd_{0.56}Se$	0.8	0.7951	0.8186
$Zn_{0.56}Cd_{0.44}Se$	1.2	1.1245	1.2111
$Zn_{0.67}Cd_{0.33}Se$	2.0	1.8271	2.0275

Table 2: Molar ratios of zinc and cadmium in undecomposed $Zn_xCd_{1-x}Se$ nanocrystals and in solution phase after photodecomposition studies measured by the atomic absorption spectroscopy (AAS) and the mercury film electrochemical technique (ECA).

Zn:Cd ratio	Zn:Cd molar ratio in nanocrystals by AAS	Zn:Cd molar ratio in nanocrystals by ECA	Zn:Cd molar ratio in solution phase by AAS	Zn:Cd molar ratio in solution phase by ECA
$Zn_{0.25}Cd_{0.75}Se$	0.1923	0.2134	0.9833	0.9733
$Zn_{0.44}Cd_{0.56}Se$	0.7355	0.7995	0.9751	0.9630
$Zn_{0.56}Cd_{0.44}Se$	1.3415	1.3897	0.9594	0.9745
$Zn_{0.67}Cd_{0.33}Se$	2.1038	2.2148	0.9821	1.0384

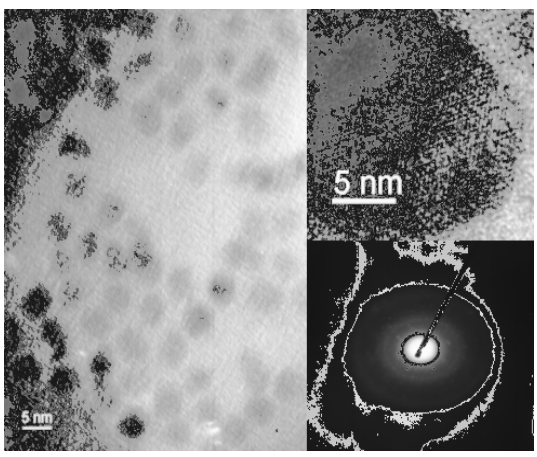

(a) 5.8 nm
$Zn_{0.25}Cd_{0.75}$**Se**

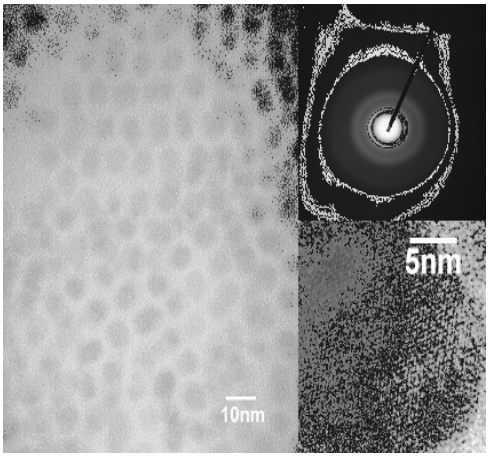

(b) 6.3 nm
$Zn_{0.44}Cd_{0.56}Se$

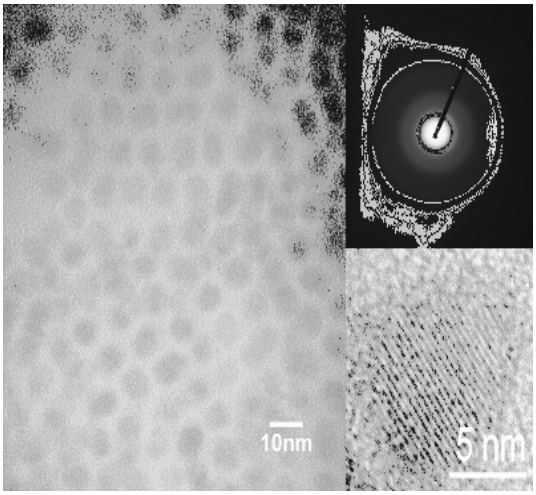

(c) 6.8 nm
$Zn_{0.56}Cd_{0.33}Se$

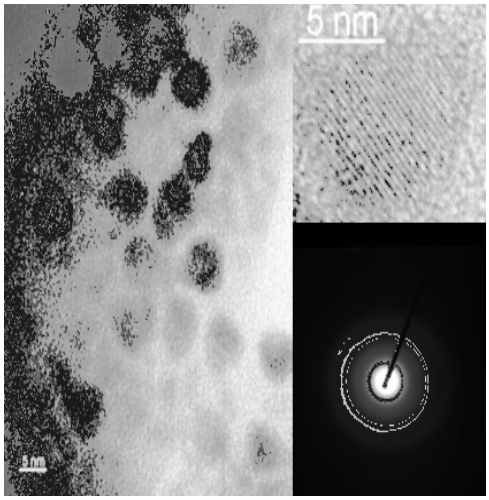

(d) 7.5 nm
$Zn_{0.67}Cd_{0.33}Se$

Figure 7: HR-TEM characterisation for $Zn_xCd_{1-x}Se$ nanocrystals with zinc mole fractions of (a) 0.25, (b) 0.44, (c) 0.56, and (d) 0.67 with diameters of about 5.8 ± 0.3 nm, 6.3 ± 0.4 nm, 6.8 ± 0.3 nm and 7.5 ± 0.5 nm determined by TEM. The mole fractions shown are those present in the preparation of the $Zn_xCd_{1-x}Se$ nanocrystals prior to photodecomposition.

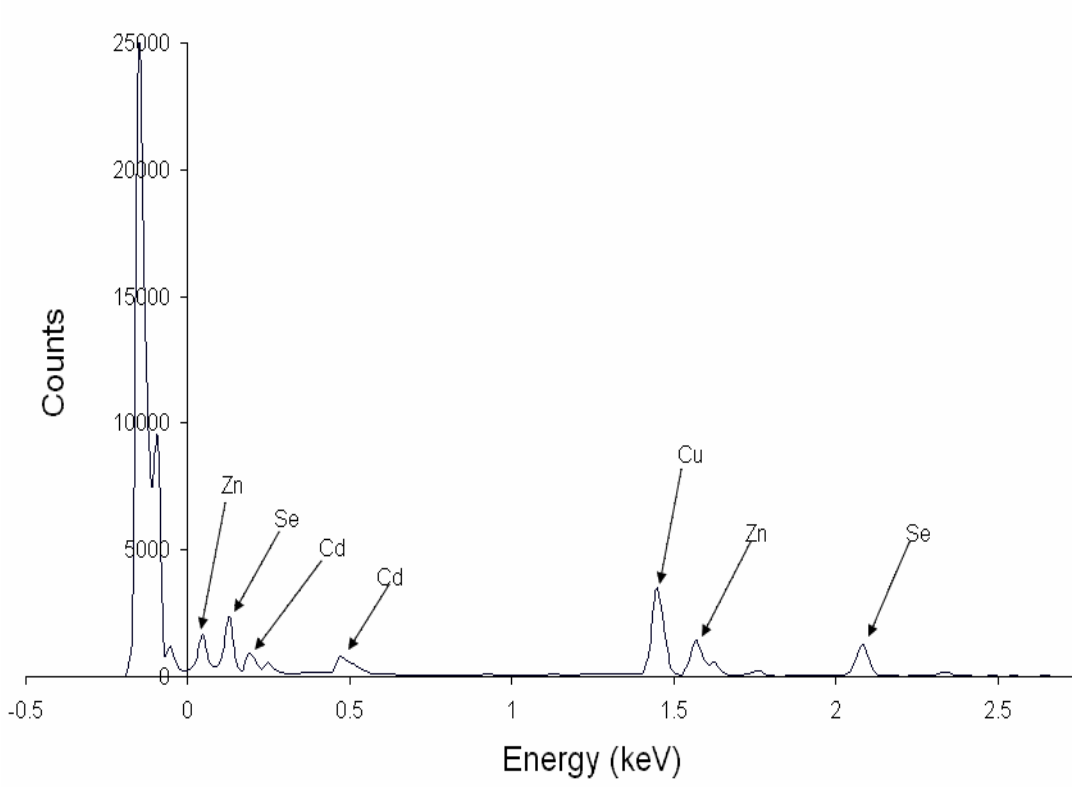

Figure 8: EDX spectra of $Zn_xCd_{1-x}Se$ nanocrystals confirming the elemental composition of cadmium, zinc and selenium present in the nanocrystal.

Table 3: Molar ratios of zinc and cadmium in $Zn_xCd_{1-x}Se$ nanocrystals and in solution with no addition of methylviologen and no exposure to light (control studies) measured by the atomic absorption spectroscopy (AAS) and the mercury film electrochemical technique (ECA).

Zn:Cd ratio	Zn:Cd molar ratio in nanocrystal by AAS	Zn:Cd molar ratio in nanocrystal by ECA	Zn:Cd molar ratio in aqueous phase by AAS	Zn:Cd molar ratio in aqueous phase by ECA
$Zn_{0.28}Cd_{0.72}Se$	0.3676	0.3889	Not detected	Not detected
$Zn_{0.44}Cd_{0.56}Se$	0.7617	0.7892	Not detected	Not detected
$Zn_{0.55}Cd_{0.45}Se$	1.1176	1.2021	Not detected	Not detected
$Zn_{0.67}Cd_{0.33}Se$	1.8181	1.9681	Not detected	Not detected

DISCUSSION

$Zn_xCd_{1-x}Se$ Nanocrystal as-prepared

It can be seen from the UV-Visible spectra in Figure 1 that there is a shift to lower wavelengths with the addition of more zinc precursor to the CdSe nuclei. The systematic composition controlled shift of the absorption onset to shorter wavelength is strong evidence for the formation of alloyed nanocrystals via the intermixing of the wider band-gap ZnSe with the narrower band gap CdSe nanocrystal, rather than the formation of CdSe and ZnSe nanocrystals (Suthan et al, 2011), or core-shell CdSe/ZnSe structures (Kippeny et al, 2008). If ZnSe nucleated separately, individual absorption peaks for the two chalcogenides would have appeared. The absence of two absorption features rules out the formation of ZnSe nanocrystals; a conclusion supported by the HR-TEM results. Also, if CdSe/ZnSe core shell nanocrystals had formed, the resulting absorption excitonic onset would have shifted to longer wavelength as compared with that of pure CdSe due to partial leakage of the exciton into the shell matrix (Dabbousi et al, 1997; Margaret et al, 1996; Reiss et al, 2002; Xiaogang et al, 1997).

The HR-TEM in Figure 7 shows nearly monodispersed $Zn_xCd_{1-x}Se$ nanocrystals, which have well-resolved lattice fringes that have remained fully crystalline upon incorporation of zinc precursor. The particle size as determined by TEM increased proportionately from 5.8 ± 0.3 to 7.5 ± 0.5 nm with an increase in zinc content from 0.25 to 0.67. Alloyed $Zn_xCd_{1-x}Se$ quantum dots were successfully prepared by the embryonic nuclei-induced alloying process (Yu et al., 2003; Zhong et al., 2004). The two-step synthetic procedure was designed to separate the CdSe nucleation process from the subsequent seeding growth of the $Zn_xCd_{1-x}Se$ quantum dots. Small CdSe nuclei seeds were made first, followed by the growth of these nuclei into $Zn_xCd_{1-x}Se$ quantum dots by incorporating zinc into the existing CdSe monomer. This synthetic strategy was highly reproducible and could be developed into a practical method for commercial applications.

Results of the elemental analysis of the $Zn_xCd_{1-x}Se$ nanocrystal solutions are given in Table 5. The ratio of Zn:Cd in the particles matched that in the reaction vessel during preparation. This was a surprising observation because for a normal co-precipitation reaction, the precipitate should have been richer in the cadmium precursor which was the more insoluble component. This could be due to the fact that ZnSe and CdSe were both very sparingly soluble in the solvents and that there was an excess of Se in the synthesis vessel, such that all the zinc and cadmium were present in the particulate form.

$Zn_xCd_{1-x}Se$ Nanocrystals after Photodecomposition

Prior to photodecomposition, the emission colours of the prepared $Zn_xCd_{1-x}Se$ solution varied from brown to blue as the zinc content in the CdSe was decreased, while after photodecomposition, the colours remained blue for all the zinc mole fractions.

There are two preconceptions that should be met for alloyed nanocrystals formation and dissolution. The first is that there is no surface segregation. This implies that there is a uniform distribution of the ions in solution thereby giving the same ratio of Cd:Zn in the solution phase and in the particles after photodecomposition. The second is that there is surface segregation in which one element is favoured at the surface. For example in a Cd_aZn_bSe nanocrystal, if Zn is the favoured component, then after formation, the Cd:Zn ratio at the surface will be less than a/b and in the core it will be greater than a/b. After photodecomposition the ratio of Cd:Zn ions in the solution phase will be less than a/b and greater than a/b in the particles. This is unlikely because if the particles are fully decomposed and then reform, no quantum dots will result.

Another possible explanation is that the particles are non-uniformly distributed within the shell, while the outer shell contains 50% of either ion. In the formation of $Cd_xZn_{1-x}Se$ alloyed nanocrystals, there is competition between the maximisation of bonding energy and the minimisation of lattice stress during thermal treatment and this determines the ratio of zinc to cadmium. As a consequence after photodecomposition the zinc fraction in particles in which $x > 0.5$ increases whilst for particles in which $x < 0.5$ it decreases. These preconceptions can only be confirmed by further experiments to determine both the mechanism by which zinc is alloyed in the CdSe nanocrystals, and also the Cd:Zn ratio in the $Zn_xCd_{1-x}Se$ quantum dots that were formed during the alloying process.

However, the results of the photodecomposition studies shown in Table 2 were different from these preconceptions. They were self-consistent, in that, a 1:1 ratio of Zn^{2+} and Cd^{2+} ions in the solution phase agreed with the change in the composition of the crystals. The results also showed that, by using photon energy of incident light and an electron scavenger, it is possible to etch larger $Zn_xCd_{1-x}Se$ quantum dots to smaller sizes.

The result of the control studies given in Table 3 showed that photo dissolution had taken place. This is because the Zn:Cd molar ratio of the $Zn_xCd_{1-x}Se$ nanocrystals obtained from the control studies were in agreement with those obtained before photodecomposition took place, and no zinc and cadmium ions were found in the aqueous phase.

Conclusion

In this paper we have shown that $Zn_xCd_{1-x}Se$ quantum dots can be prepared by the embryonic nuclei-induced alloying technique. The prepared $Zn_xCd_{1-x}Se$ quantum dots had different UV vis absorption wavelength greater than 450 nm; they had well-resolved lattice fringes; and they also remained fully crystalline upon zinc incorporation into the CdSe nanocrystals. The photodecomposition study clearly showed a lowering of the maximum absorption wavelengths to less than 450 nm due to size reduction of the $Zn_xCd_{1-x}Se$ quantum dots. We believe that this preliminary characteristic observation on the reduced maximum absorption wavelength on the $Zn_xCd_{1-x}Se$ quantum dots will be helpful to explore the biomedical imaging performance of the quantum dots. However toxicity studies on these quantum dots are recommended before injecting them into injured tissues.

ACKNOWLEDGMENTS

Financial support from the School of Chemistry and the University of Bristol is acknowledged. The authors thank Dr Roy Hughes of the Bristol Colloid Centre in the University of Bristol and Dr. D. Jason Riley of the Department of Materials at Imperial College London for their interest in and contributions to this work. A Commonwealth fellowship tenable in the United Kingdom enabled the finalisation of the write-up.

REFERENCES

Artemyev MV, Woggon U, Wannemacher R, Jaschinski H, Langbein W. 2001. Light trapped in a photonic dot: Microspheres act as cavity for quantum dot emission. *Nano Lett.*, **1**: 309-393.

Bruchez MP, Moronne M, Gin P, Weiss S, Alivisatos AP. 1998. Semiconductor nano crystals as fluorescent biological labels. *Science*, **281:** 2013-2016.

Chan WCM, Nie SM. 1998. Quantum dot bioconjugates for ultrasensitive nonisotropic detection. *Science*, **281**: 2016-2018.

Colvin VL, Schlamp MC, Alivisatos AP. 1994. Light-emitting-diodes made from cadmium selenide nanocrystals and a semiconducting polymer. *Nature*, **370**: 354-357.

Gao M, Lesser C, Kirstein S, Mohwald H, Rogach AL, Weller H. 2000. Electroluminence of different colours from poly-cation CdTe nanocrystal self-assembled films. *J. Appl. Phys.*, **87**: 2297-2302.

Harrison MT, Kershaw SV, Burt MG, Eychmuller A, Weller H, Rogach AL. 2000. Wet chemical synthesis and spectroscopic study of CdHgTe nanocrystals with strong near-infrared luminescence. *Mater. Sci. Eng. B*, **69**: 355-360.

Jaiswal JK, Mattoussi H, Mauro JM, Simon SM. 2003. Long-term multiple imaging of live cells using quantum dot bioconjugates. *Biotechnology*, **21**: 47-51.

Kippeny TC, Bowers MJ, Dukes AD, McBride JR, Orndorff RL, Garrett MD, Rosenthal SJ. 2008. Effect of surface passivation on the exciton dynamics of CdSe nanocrystals as observed by ultrafast fluorescence upconversion spectroscopy. *J. Chem. Phys.* **128**: 084713, doi:10.1063

Klimov VI, Mikhailovsky AA, Xu S, Malko A, Hollingsworth JA, Leatherdale CA, Eisler HJ, Bawendi MG. 2000. Optical gain and stimulated emission nanocrystals. *Science*. **290**: 314-317.

Korgel BA and Monbouquette HG. 2000. Controlled synthesis of mixed core and layered (Zn, Cd)S and (Hg, Cd)S nanocrystals within phosphatidylcholine vesicles. *Langmuir*. **16**:3588-3594.

Kovalevskij V, Gulbinas V, Piskarskas A, Hines, MA, Scholes GD. 2004. Surface passivation in CdSe nanocrystal-polymer films revealed by ultrafast exciton relaxation dynamics. *Phys. Stat. Sol. (b.)* **241**(8): 1986-1993

Kulkarni SK, Winkler U, Deshmukh N, Borse PH, Fink R,Umbach E, 2001. Investigations of chemically capped CdS, ZnS and ZnCdS nanoparticles. *Appl. Surf. Sci.* **169**: 438-446.

Margaret AH, Philippe GS. 1996. Synthesis and characterisation of strongly luminescent ZnS-capped CdSe nanocrystals. *J. Phys. Chem.*, **100**: 468-471.

Murray CB, Norris DJ, Bawendi MG. 1993. Synthesis and characterization of nearly monodisperse CdE (E=sulpur, selenium,tellurium) semiconductor nanocrystallites. *J. Am. Chem. Soc.*, **115**: 8706-8715.

Peng X. 2002. Green chemical approaches toward high-quality semiconductor nanocrystals. *Chem. Eur. J.* **8**: 334-339.

Peng ZA, Peng X. 2001. Mechanism of shape evaluation of CdSe. *J. Am. Chem. Soc.*, **123**: 183-184.

Petrov DV, Santos BS, Pereira GAL, Donega CDM. 2002. Size and band-gap dependences of hyperpolarizability of $Cd_xZn_{1-x}S$ nanocrystals. *J. Phys. Chem. B*, **106**: 5325-5334.

Qu LH, Peng XG. 2002. Control of photoluminicence properties of CdSe nanocrystals in growth. *J. Am. Chem. Soc.*, **124**: 2049-2055

Qu L, Peng ZA, Peng X. 2001. Study of growth kinetics of CdSe nanocrystals with a new model. *Nano Lett.*, **1:** 333-337.

Reiss P, Bleuse J, Adam P. 2002. Highly luminescent CdSe/ZnSe core/shell nanocrystals of low size dispersion. *Nano Lett.*, **7**: 781-784.

Schlamp MC, Peng X, Alivisatos AP. 1997. Improved efficiencies in light-emitting diodes made with CdSe (CdS) core/shell type nanocrystals and a semiconducting polymer. *J. Appl. Phys.*, **82**: 58375842.

Suthan NJK, Perumal K, Suthagar J. 2011. Preparation and properties of zinc doped cadmium selenide compounds by E-beam evaporation. *J. Nano. Electron. Phys*., **3**(3): 5- 14.

Tessler N, Medvedev V, Kazes M, Kan SH, Banin U. 2002. Efficient near-infrared

polymer nanocrystals light-emitting diodes. *Science,* **295**: 1506-1508.

Wang W, Germanenko I, El-Shall MS. 2002. Room-temperature synthesis and characterization of nanocrystalline CdS, ZnS, and $Cd_xZn_{1-x}S$. *Chem. Mater.,* **14**(7): 3028-3033.

Wu X, Liu H, Liu J, Haley KN, Treadway JA, Larson JP, Ge N, Peale F, Brucher MP. 2003. Immunofluorescent labelling of cancer marker Her2 and other cellular targets with semiconductor quantum dots. *Nature Biotechnology,* **21**: 41-46.

Xiaogang P, Michael CS, Andreas VK, Alivisatos AP. 1997. Epitaxial growth of highly luminescent CdSe/CdS core/shell nanocrystals with photostability and electronic accessibility. *J. Am. Chem. Soc.*, **119**: 7019-7029.

Yu WW, Qu LH, Guo WZ, Peng XG. 2003. Experimental determination of the extinction coefficient CdSe and CdS nanocrystals. *Chem. Mater.*, **15**: 2854-2860.

Zhong X, Zhang Z, Liu S, Han M, Knoll W. 2004. Embryonic nuclei-induced alloying process for the reproducible synthesis of blue-emitting $Zn_xCd_{1-x}Se$ nanocrystals with long-time thermal stability in size distribution and emission wavelength. *J. Phys. Chem. B*, **108**: 15552-15559.